# The b-quark mass from non-perturbative $N_f = 2$ Heavy Quark Effective Theory at O(1/$m_h$)

## ALPHA Collaboration

Fabio Bernardoni [a], Benoît Blossier [b], John Bulava [c], Michele Della Morte [d], Patrick Fritzsch [e,*], Nicolas Garron [c], Antoine Gérardin [b], Jochen Heitger [f], Georg von Hippel [g], Hubert Simma [a], Rainer Sommer [a]

[a] *NIC @ DESY, Platanenallee 6, 15738 Zeuthen, Germany*
[b] *Laboratoire de Physique Théorique, Université Paris XI, 91405 Orsay Cedex, France*
[c] *School of Mathematics, Trinity College, Dublin 2, Ireland*
[d] *IFIC and CSIC, Calle Catedrático José Beltran 2, 46980 Paterna, Valencia, Spain*
[e] *Institut für Physik, Humboldt-Universität zu Berlin, Newtonstr. 15, 12489 Berlin, Germany*
[f] *Institut für Theoretische Physik, Universität Münster, Wilhelm-Klemm-Str. 9, 48149 Münster, Germany*
[g] *PRISMA Cluster of Excellence, Institut für Kernphysik, University of Mainz, Becherweg 45, 55099 Mainz, Germany*

## ARTICLE INFO

## ABSTRACT

We report our final estimate of the b-quark mass from $N_f = 2$ lattice QCD simulations using Heavy Quark Effective Theory non-perturbatively matched to QCD at O(1/$m_h$). Treating systematic and statistical errors in a conservative manner, we obtain $\overline{m}_b^{\overline{\text{MS}}}(2 \text{ GeV}) = 4.88(15)$ GeV after an extrapolation to the physical point.

## 1. Introduction

The masses of the quarks are among the fundamental parameters of the Standard Model (SM), and as such hold considerable interest. Heavy quark masses, in particular, enter as parameters in various perturbative predictions of interesting decay rates, e.g. $B \to X_s \gamma$ or inclusive $B \to u$ or $B \to c$ rates. Such decays yield useful constraints for the CKM matrix and, in principle, options to obtain hints for physics beyond the Standard Model. It is therefore desirable to minimize the uncertainty in $m_b$ entering these predictions.

The b-quark mass also enters the prediction for the cross section of the $H \to b\bar{b}$ decay, which is the mode with the largest branching ratio for an SM-like Higgs with a mass of 126 GeV. In the future, tests of this coupling will help providing further characterizations of the new boson.

The most accurate determinations of the b-quark mass reported in the PDG review [1–25] come from comparisons of experimental results for the $e^+ e^- \to b\bar{b}$ cross section to theoretical predictions from perturbation theory and sum-rules.

Like each of these approaches, the first-principles determination of $m_b$ from lattice field theory has its own difficulties. Relativistic b-quarks cannot yet be reliably simulated on the lattice as their Compton wavelength is much shorter than any lattice spacing which can be currently reached in large-volume simulations. To circumvent this limitation, two approaches have been used, viz. extrapolating simulation results obtained in the vicinity of the charm quark mass to the b-quark region [24–28], and the use of effective field theories, such as NRQCD [29,30]. The approach of the ALPHA Collaboration is based on Heavy Quark Effective Theory (HQET) [31–34], which provides a description of heavy quarks in the context of heavy–light mesons that can be employed in lattice QCD simulations if the parameters of HQET are determined by matching HQET to QCD non-perturbatively [35,36]. The matching at order O(1/$m_h$) has been performed in both the quenched ($N_f = 0$) and the $N_f = 2$ theories by our collaboration [37,38]. The

lattice approach in general offers the unique opportunity to study the $N_f$-dependence of the b-quark mass. We will further discuss that in the conclusions.

In this Letter, we present our results for the mass of the b-quark from simulations of non-perturbative $N_f = 2$ HQET. In Section 2, we briefly review the methods employed before presenting the results in Section 3. Section 4 contains our conclusions.

## 2. Methodological background

HQET on the lattice constitutes a theoretically sound approach to heavy quark physics by expanding QCD correlation functions into power series in $1/m_h$ around the static limit $m_h \to \infty$, which is non-perturbatively renormalizable, so that the continuum limit can always be taken.

Following the strategy described in [35,39] and previously applied to calculate $m_b$ in the quenched approximation [36], we write the HQET action at O$(1/m_h)$ as

$$S_{HQET} = a^4 \sum_x \{ \mathcal{L}_{stat}(x) - \omega_{kin} \mathcal{O}_{kin}(x) - \omega_{spin} \mathcal{O}_{spin}(x) \}, \quad (2.1)$$

$$\mathcal{L}_{stat}(x) = \overline{\psi}_h(x)(D_0 + m_{bare})\psi_h(x), \quad (2.2)$$

$$\mathcal{O}_{kin}(x) = \overline{\psi}_h(x)\mathbf{D}^2\psi_h(x), \quad (2.3)$$

$$\mathcal{O}_{spin}(x) = \overline{\psi}_h(x)\boldsymbol{\sigma} \cdot \mathbf{B}\psi_h(x), \quad (2.4)$$

where the heavy quark spinor field $\psi_h$ obeys $\frac{1+\gamma_0}{2}\psi_h = \psi_h$, $m_{bare}$ is the bare heavy quark mass absorbing the power-divergences of the self-energy in the static approximation, and the parameters $\omega_{kin}$ and $\omega_{spin}$ are formally of order $1/m_h$ and have been previously determined in [38]. The O$(1/m_h)$ terms in (2.1) are treated as operator insertions in static correlation functions:

$$\langle O \rangle = \langle O \rangle_{stat} + \omega_{kin} a^4 \sum_x \langle O \mathcal{O}_{kin}(x) \rangle_{stat}$$
$$+ \omega_{spin} a^4 \sum_x \langle O \mathcal{O}_{spin}(x) \rangle_{stat} \quad (2.5)$$

for the expectation value of some multilocal fields $O$, where $\langle O \rangle_{stat}$ is the expectation value of $O$ determined in the static theory. A significant improvement in the signal-to-noise ratio of heavy–light correlation functions can be achieved by defining the covariant backward time derivative $D_0 f(x) = (f(x) - U^\dagger(x - a\hat{0}, 0) \times f(x - a\hat{0}))/a$ in terms of a suitably smeared link instead of the bare link $U(x, 0)$. Each smearing prescription constitutes a separate lattice action; here we have employed both the HYP1 and HYP2 actions [40–42].

To reliably extract hadronic quantities, we have to pay particular attention to unwanted contributions from excited states. The variational method, which has become a standard tool for analyzing hadronic spectra in lattice QCD, starts from correlator matrices

$$C_{ij}^{stat}(t) = \sum_{x,\mathbf{y}} \langle O_i(x_0 + t, \mathbf{y}) O_j^*(x) \rangle_{stat},$$

$$C_{ij}^{kin/spin}(t) = \sum_{x,\mathbf{y},z} \langle O_i(x_0 + t, \mathbf{y}) O_j^*(x) \mathcal{O}_{kin/spin}(z) \rangle_{stat}, \quad (2.6)$$

for a suitably chosen basis of interpolating fields $O_i$, $i = 1, \ldots, N$. The main ingredient is to solve the generalized eigenvalue problem (GEVP) in the static limit

$$C^{stat}(t) v_n^{stat}(t, t_0) = \lambda_n^{stat}(t, t_0) C^{stat}(t_0) v_n^{stat}(t, t_0),$$
$$n = 1, \ldots, N, \ t > t_0. \quad (2.7)$$

Indeed, by exploiting the orthogonality property of the eigenvectors

$$\left( v_m^{stat}(t, t_0), C^{stat}(t_0) v_n^{stat}(t, t_0) \right) \propto \delta_{nm}$$

one can show that the O$(1/m_h)$ corrections to the energy levels depend only on the static generalized eigenvalues $\lambda_n^{stat}(t, t_0)$, the eigenvectors $v_n^{stat}(t, t_0)$, and the O$(1/m_h)$ correlators $C^{kin/spin}(t)$ [43], in analogy with perturbation theory in quantum mechanics. At large times $t$ and $t_0$ satisfying $t_0 \geqslant t/2$, the asymptotic behaviour is then known to be [43]

$$E_n^{eff,stat}(t, t_0) = E_n^{stat} + \beta_n^{stat} e^{-\Delta E_{N+1,n}^{stat} t} + \cdots, \quad (2.8)$$

$$E_n^{eff,(1/m)}(t, t_0) = E_n^{(1/m)} + \left[ \beta_n^{(1/m)} - \beta_n^{stat} t \Delta E_{N+1,n}^{(1/m)} \right] e^{-\Delta E_{N+1,n}^{stat} t}$$
$$+ \cdots, \quad (2.9)$$

with $\Delta E_{m,n} = E_m - E_n$. The time intervals over which we fit the energy plateaux are chosen so as to minimize the systematic error from the excited states while keeping the statistical error under control.

Finally, the mass of the B-meson to O$(1/m_h)$ is given by ($E^x \equiv E_1^x$)

$$m_B = m_{bare} + E^{stat} + \omega_{kin} E^{kin} + \omega_{spin} E^{spin} \quad (2.10)$$

and it remains to perform the chiral and continuum extrapolation and to solve the equation $m_B(m_h = m_b) = m_B^{exp}$ by an interpolation.

## 3. Simulation details and results

### 3.1. Ensembles used

Our measurements are carried out on a subset of the CLS (Coordinated Lattice Simulations) ensembles, which have been generated using either the DD-HMC [44–47] or the MP-HMC [48] algorithm, using the Wilson plaquette action [49] and $N_f = 2$ flavours of non-perturbatively O$(a)$ improved Wilson quarks [50,51]. An overview of the simulation parameters of the ensembles used is given in Table 1. In order to suppress finite-size effects, we consider only ensembles satisfying $m_\pi L > 4.0$. The light valence quarks are equal to the sea quarks, and the (quenched) b-quark is treated by HQET.

In order to control the statistical error in a reliable fashion, we make use of the method of [53] as improved by [52] to estimate the effect of long-term autocorrelations due to the coupling of our observables to the slow modes of the Markov chain, decaying as $\sim \exp(-\tau/\tau_{exp})$ in Monte Carlo simulation time $\tau$. The propagation of these effects through to the continuum-extrapolated result at the physical pion mass is carried out iterating the formulae of [52].

### 3.2. Lattice spacings

The lattice spacings $a$, pion masses $m_\pi$ and pion decay constants $f_\pi$ on the CLS ensembles used here are taken from an update [54] of the analysis in [55] with increased statistics and including additional ensembles. They read

$$a = 0.04831(38) \text{ fm} \quad \text{at } \beta = 5.5,$$
$$a = 0.06531(60) \text{ fm} \quad \text{at } \beta = 5.3,$$
$$a = 0.07513(79) \text{ fm} \quad \text{at } \beta = 5.2, \quad (3.1)$$

and result from setting the scale via the kaon decay constant, $f_K = 155$ MeV. With the updated values of $af_K$ we follow the lines of [55] and re-evaluate

$$L_1 f_K = \lim_{a \to 0} [L_1/a][af_K] = 0.312(8) \quad (3.2)$$

**Table 1**

Details of the CLS ensembles used: bare coupling $\beta = 6/g_0^2$, lattice spacing $a$, spatial extent $L$ in lattice units ($T = 2L$), pion mass $m_\pi$, $m_\pi L$, number of configurations employed, and number of configurations employed normalized in units of the exponential autocorrelation time $\tau_{\exp}$ as estimated in [52]. Additionally, we specify the CLS label id and the Gaussian smearing parameters $R_k$ used to build different interpolating fields as described in the text.

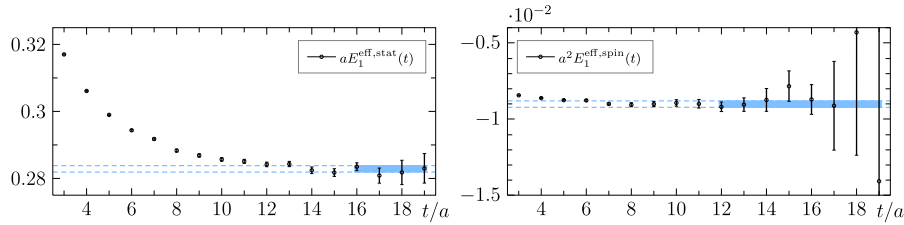| $\beta$ | $a$ [fm] | $L/a$ | $m_\pi$ [MeV] | $m_\pi L$ | #cfgs | $\frac{\text{\#cfgs}}{\tau_{\exp}}$ | id | $\{R_1, R_2, R_3\}$ |
|---|---|---|---|---|---|---|---|---|
| 5.2 | 0.075 | 32 | 380 | 4.7 | 1012 | 122 | A4 | {15, 60, 155} |
| | | 32 | 330 | 4.0 | 1001 | 164 | A5 | |
| | | 48 | 280 | 5.2 | 636 | 52 | B6 | |
| 5.3 | 0.065 | 32 | 440 | 4.7 | 1000 | 120 | E5 | {22, 90, 225} |
| | | 48 | 310 | 5.0 | 500 | 30 | F6 | |
| | | 48 | 270 | 4.3 | 602 | 36 | F7 | |
| | | 64 | 190 | 4.1 | 410 | 17 | G8 | |
| 5.5 | 0.048 | 48 | 440 | 5.2 | 477 | 4.2 | N5 | {33, 135, 338} |
| | | 48 | 340 | 4.0 | 950 | 38 | N6 | |
| | | 64 | 270 | 4.2 | 980 | 20 | O7 | |



**Fig. 1.** Illustration of typical plateaux for the ground state static energy (left panel) and the O($1/m_b$) chromomagnetic energy (right); the CLS ensemble shown here is N6 ($a = 0.048$ fm, $m_\pi = 340$ MeV).

that is needed to convert the b-quark mass into physical units later on. The length scale $L_1$ originates from the non-perturbative finite-volume matching step used to determine the HQET parameters [38].

### 3.3. Basis of B-meson interpolating fields

Our basis of $N = 3$ operators is given by

$$O_k(x) = \overline{\psi}_{\text{h}}(x)\gamma_0\gamma_5\psi_1^{(k)}(x), \quad k = 1, \ldots, N, \quad (3.3)$$

where $\psi_{\text{h}}(x)$ is the static quark field, and different levels of Gaussian smearing [56] with a triply (spatially) APE smeared [57,58] covariant Laplacian $\Delta$ are applied to the relativistic quark field

$$\psi_1^{(k)}(x) = \left(1 + \kappa_G a^2 \Delta\right)^{R_k}\psi_1(x). \quad (3.4)$$

Our smearing parameters $\kappa_G = 0.1$ and $R_k$, collected in Table 1, are chosen so as to use approximately the same sequence of physical radii $r_k = 2a\sqrt{\kappa_G R_k}$ at each value of the lattice spacing. In extracting our estimates for the energies $E_1^{\text{stat,kin,spin}}$ from the GEVP, the time intervals $[t_{\min}, t_{\max}]$ over which we fit the plateaux are chosen so as

$$r(t_{\min}) = \frac{|A(t_{\min}) - A(t_{\min} - \delta)|}{\sqrt{\sigma^2(t_{\min}) + \sigma^2(t_{\min} - \delta)}} \leqslant 3, \quad (3.5)$$

where $A$ is the plateau average, $\sigma$ is the statistical error, $\delta = 2/(E_{N+1}^{\text{stat}} - E_1^{\text{stat}}) \sim 0.3$ fm, and $t_{\max}$ is fixed to $\sim 0.9$ fm. This will assure that our selection criterion $\sigma_{\text{sys}} \leqslant \sigma/3$ is satisfied [59], where $\sigma_{\text{sys}} \propto \exp[-(E_{N+1} - E_1)t_{\min}]$. An illustration of two typical plateaux of $E_1^{\text{stat}}$ and $E_1^{\text{spin}}$ is shown in Fig. 1.

### 3.4. Determination of the b-quark mass

The mass of the B-meson to static order is given by

$$m_{\text{B}}^{\text{stat}} = m_{\text{bare}}^{\text{stat}} + E^{\text{stat}} \quad (3.6)$$

while the main formula at O($1/m_b$) was given in Eq. (2.10). The HQET parameters $m_{\text{bare}}^{\text{stat}}$, $m_{\text{bare}}$, $\omega_{\text{kin}}$ and $\omega_{\text{spin}}$ depend on the renormalization group invariant (RGI) heavy quark mass $M$ (defined below) and the lattice spacing $a$. We parameterize this dependence by the dimensionless variable $z = ML_1$ and $a$, where $L_1$ is kept fixed. It is implicitly defined by the renormalized coupling in the Schrödinger Functional (SF) scheme via $\bar{g}^2(L_1/2) = 2.989$ [38]. Apart from $a$, the large-volume observables $E^{\text{x}}$ depend on the light quark mass which we parameterize through $m_\pi$. Thus $m_{\text{B},\delta}$, computed with discretization HYP1 for $\delta = 1$ and HYP2 for $\delta = 2$, are functions of $z$, $m_\pi$ and $a$. Their values are listed in Table 2.

Once $m_{\text{B},\delta}$ have been computed for a set of $z$ spanning a range of heavy quark masses containing the b-quark mass, we perform a combined chiral and continuum extrapolation to obtain $m_{\text{B}}(z, m_\pi^{\exp}) \equiv m_{\text{B},\delta}(z, m_\pi^{\exp}, 0)$, using $m_\pi^{\exp} = 134.98$ MeV [1]. Considering that the O($a$) improvement was performed non-perturbatively but neglecting O($a/m_b$) effects,[1] the NLO formula from HMChPT reads [60]

$$m_{\text{B},\delta}^{\text{sub}}(z, y, a) = B(z) + C(y - y^{\exp}) + D_\delta a^2, \quad y \equiv \frac{m_\pi^2}{8\pi^2 f_\pi^2}, \quad (3.7)$$

where in

$$m_{\text{B},\delta}^{\text{sub}}(z, y, a) \equiv m_{\text{B},\delta}(z, m_\pi, a) + \frac{3\hat{g}^2}{16\pi}\left(\frac{m_\pi^3}{f_\pi^2} - \frac{(m_\pi^{\exp})^3}{(f_\pi^{\exp})^2}\right) \quad (3.8)$$

the leading non-analytic term of HMChPT has been subtracted. The $B^*B\pi$ coupling $\hat{g} = 0.489(32)$ has been determined recently [61] and the variable $y$ is identical to $\tilde{y}_1$ introduced in [55]. We use the convention where the pion decay constant is $f_\pi^{\exp} = 130.4$ MeV. The extrapolation (3.7) is shown in Fig. 2 (left) for three values of $z$ in the vicinity of $z_b = M_b L_1$ we are aiming at. Its result, $B(z) = m_{\text{B},\delta}(z, m_\pi^{\exp}, 0)$, is given in Table 2. As shown in Fig. 2

---

[1] Accounting for an $a/m_b$ has little effect. Adding a term $F_\delta \cdot (a/m_b)$ to Eq. (3.7) does not change the unnormalized $\chi^2$. For instance, the fitting parameter $B(z)|_{z=13}$ changes to 5227(79) MeV and Eq. (3.10) would read $z_b = 13.18(27)(13)$.

**Table 2**

Raw data of $m_{B,\delta}(z, m_\pi, a)$ in MeV for all ensembles (id), $z$ and HYP actions considered in this work. In the last row we report $B(z) \equiv m_{B,\delta}^{sub}(z, m_\pi^{exp}, 0)$ for the $z$ that were used in the quadratic interpolation to fix $z_b$ using Eq. (3.9).

| id | $y$ | $z = 11$ | | $z = 13$ | | $z = 15$ | |
|----|-----|----------|----------|----------|----------|----------|----------|
| | | HYP1 | HYP2 | HYP1 | HYP2 | HYP1 | HYP2 |
| A4 | 0.0771(14) | 4434(62) | 4454(62) | 5024(70) | 5042(70) | 5597(78) | 5613(78) |
| A5 | 0.0624(13) | 4419(62) | 4440(62) | 5010(70) | 5028(70) | 5583(78) | 5600(78) |
| B6 | 0.0484(9) | 4398(62) | 4420(62) | 4988(70) | 5008(70) | 5562(78) | 5579(78) |
| E5 | 0.0926(15) | 4474(59) | 4492(59) | 5069(66) | 5084(66) | 5646(73) | 5661(73) |
| F6 | 0.0562(9) | 4436(59) | 4452(58) | 5031(66) | 5046(66) | 5609(73) | 5622(73) |
| F7 | 0.0449(7) | 4431(58) | 4444(58) | 5026(65) | 5037(65) | 5603(73) | 5613(73) |
| G8 | 0.0260(5) | 4415(59) | 4434(59) | 5010(66) | 5027(66) | 5589(73) | 5603(73) |
| N5 | 0.0940(24) | 4586(57) | 4594(57) | 5193(64) | 5200(63) | 5783(71) | 5789(70) |
| N6 | 0.0662(10) | 4563(57) | 4568(56) | 5169(63) | 5174(63) | 5759(70) | 5763(70) |
| O7 | 0.0447(7) | 4539(56) | 4555(56) | 5147(63) | 5161(63) | 5737(69) | 5750(70) |
| $B(z)$ | | 4610(57) | | 5207(63) | | 5787(69) | |
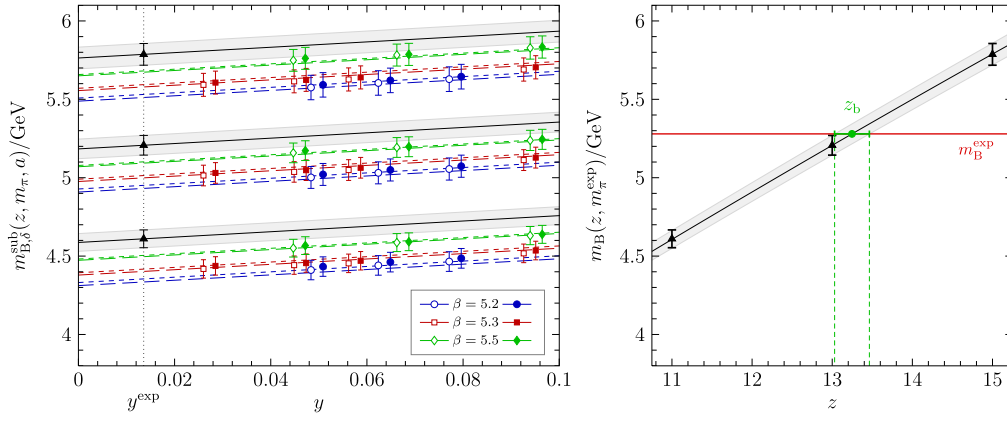


**Fig. 2.** (Left) Chiral and continuum extrapolation of $m_{B,\delta}^{sub}(z, y, a)$ for the $z$ used in the determination of $z_b$. Open/filled symbols refer to HYP1/HYP2 data points as do long/short dashed curves, respectively. (Right) Interpolation to $z_b$ by imposing Eq. (3.9).

(right) the corresponding dependence of $m_B$ on $z$ at the physical point is nearly linear, indicating that the HQET expansion is precise for this observable. Nevertheless, we perform a quadratic interpolation of $m_B(z, m_\pi^{exp}, 0)$ and fix $z_b$ by imposing the experimental value for the B-meson mass,

$$m_B(z, m_\pi^{exp}, 0)\big|_{z=z_b} \equiv m_B^{exp}. \tag{3.9}$$

We take $m_B^{exp} = 5.2795$ GeV [1] and obtain

$$z_b = 13.25(22)(13)_z, \tag{3.10}$$

where the first error is statistical and in particular contains the error from the combined chiral and continuum extrapolation, whereas the second error is the uncertainty of $h(L_0)$ defined in (A.6). It is due to the non-perturbative quark mass renormalization in QCD [38]. To give the RGI b-quark mass in physical units we combine (3.10) and (3.2) to solve the relation $z_b = L_1 M_b$ for $M_b$. According to $M_b = z_b/[L_1 f_K] \cdot f_K$ we finally obtain our main result[2]

$$M_b = 6.58(17) \text{ GeV}. \tag{3.11}$$

Since in the literature it is more common to compare masses in the $\overline{\text{MS}}$ scheme, we convert our result (3.11) and give its value $\overline{m}_b^{\overline{\text{MS}}}$ at the scale $\mu = \overline{m}_b^{\overline{\text{MS}}}$ as well as at $\mu = 2$ GeV. We use

$$\overline{m}_b^{\overline{\text{MS}}}(\overline{m}_b^{\overline{\text{MS}}}) = M_b \cdot \rho(M_b/\Lambda_{\overline{\text{MS}}}), \tag{3.12}$$

---

[2] We follow the notation of Gasser and Leutwyler [62] for the definition of the RGI mass, $M = \lim_{\mu \to \infty} (2b_0 \bar{g}^2(\mu))^{-d_0/(2b_0)} \overline{m}(\mu)$, where $b_0 = (11 - 2N_f/3)(4\pi)^{-2}$ and $d_0 = 8(4\pi)^{-2}$.

with a conversion function $\rho(r)$ that can be evaluated accurately using the known 4-loop anomalous dimensions of quark masses and coupling [63,64]. It is described in more detail in Appendix A. The ratio $r_b = M_b/\Lambda_{\overline{\text{MS}}}$ is computed from our value of $z_b$ and the ALPHA Collaboration results for non-perturbative quark mass renormalization [65]. We find $r_b = 21.1(13)$, $\rho(r_b) = 0.640(6)$ and

$$\overline{m}_b^{\overline{\text{MS}}}(2 \text{ GeV}) = 4.88(15) \text{ GeV},$$

$$\overline{m}_b^{\overline{\text{MS}}}(\overline{m}_b^{\overline{\text{MS}}}) = 4.21(11) \text{ GeV}. \tag{3.13}$$

We emphasize that this is the mass in the theory with two dynamical quark-flavours, the b-quark is quenched, a completely well defined approximation for a heavy quark. In particular also the function $\rho(r)$ refers to $N_f = 2$.

To have an idea of the magnitude of $O(1/m_b)$ corrections to the b-quark mass one must repeat the above computation in the static limit. The reason is that the $1/m$ contribution $\omega_{kin}E^{kin} + \omega_{spin}E^{spin}$ is divergent in the continuum limit; only the combination with $m_{bare}$ in Eq. (2.10) is finite. The HQET parameter $m_{bare}^{stat}$ was determined by matching the static theory with QCD as described in [38]. By repeating the same steps as for the NLO case we obtain

$$z_b^{stat} = 13.24(21)(13)_z, \qquad M_b^{stat} = 6.57(17) \text{ GeV}, \tag{3.14}$$

which after conversion to the $\overline{\text{MS}}$ scheme gives

$$\left[\overline{m}_b^{\overline{\text{MS}}}(\overline{m}_b^{\overline{\text{MS}}})\right]^{stat} = 4.21(11) \text{ GeV}. \tag{3.15}$$

The result of the combined chiral and continuum extrapolation of $m_B$ in the static limit, as well as the quadratic interpolation

**Table 3**

Partial contributions $(\sigma_i/\sigma)^2$ to the accumulated error $\sigma$ of $z_b$. Only error sources contributing with a relative squared uncertainty $(\sigma_i/\sigma)^2 > 0.5\%$ are listed. The ensemble A3 did not appear in Table 1 since it enters through the scale setting procedure [54,55] only.

| Source i | A3 | G8 | N5 | N6 | O7 | $Z_A$ | $\omega^{\mathrm{HQET}}$ |
|---|---|---|---|---|---|---|---|
| $(\sigma_i/\sigma)^2$ [%] | 1.2 | 0.9 | 2.6 | 5.9 | 5.6 | 20.6 | 61.6 |

in $z$ to obtain $z_b^{\mathrm{stat}}$ are very similar to those obtained at next-to-leading order. The small differences observed between the results in (3.10)–(3.11) and (3.14) show that for this observable the HQET expansion is very precise, making us confident that $O(1/m_b^2)$ corrections are negligible with present accuracy. Indeed, the smallness of the $1/m_b$ terms is known with much higher accuracy than (3.10) suggests, e.g., $z_b^{(1/m)} \equiv z_b - z_b^{\mathrm{stat}} = -0.008(51)$.

We conclude this section by analyzing the error budget for $z_b$. As can be seen in Table 3 approximately 62% of the contribution to the square of the error comes from the HQET parameters. Another $\sim 21\%$ comes from the relativistic $Z_A$ that affects the computation of $z_b$ through the scale setting, while only the residual $\sim 17\%$ comes from the computation of the HQET matrix elements. In this respect the largest contribution comes from the ensembles at $\beta = 5.5$, that are more affected by long-term autocorrelations (critical slowing down).

## 4. Discussion and conclusions

Using non-perturbatively matched and renormalized HQET in $N_f = 2$ lattice QCD, we have determined the mass of the b-quark with essentially controlled systematic errors: in particular, the renormalization is carried out without recourse to perturbation theory and the continuum limit is taken. An irreducible systematic error which remains is a $\Delta m_b/m_b \sim (\Lambda/m_b)^3$ relative error due to the truncation of the HQET expansion at order $\Lambda^2/m_b$. However, with a typical scale of $\Lambda = 500$ MeV one obtains a permille-sized truncation error, which is completely negligible with today's accuracy. The estimate is supported by the fact that we do not see any difference between our static result and the one including the $\Lambda^2/m_b$ terms. Furthermore, according to previous experience an effective scale of around $\Lambda = 500$ MeV seems to govern the expansion [38,59,66].

Our results,

$$M_b|_{N_f=2} = 6.58(17) \text{ GeV}, \tag{4.1}$$

$$\overline{m}_b^{\overline{\mathrm{MS}}}(2 \text{ GeV})|_{N_f=2} = 4.88(15) \text{ GeV}, \tag{4.2}$$

are in agreement with the $N_f = 2$ results of [28] who cite a similar error, but use a completely different approach. We compare to the quenched approximation and to the PDG values in Table 4. There is little dependence of $\overline{m}_b^{\overline{\mathrm{MS}}}(\mu)$ on the number of flavours for $N_f = 0, 2, 5$ and for typical values of $\mu$ between $\overline{m}_b^{\overline{\mathrm{MS}}}$ itself and 2 GeV.

In particular at the lower scale of 2 GeV, where the apparent convergence of perturbation theory is still quite good, a flavour number dependence of the mass of the b-quark is not detectable at all. In hindsight, this is rather plausible as we match our effective theories (albeit with only $N_f = 0, 2$ dynamical flavours) to the real world data at low energies. Indeed, precisely speaking the above statements refer to the theories renormalized by fixing the B-meson mass to its physical value and setting the overall energy scale through the kaon decay constant [55] or roughly equivalent the pion decay constant [54].[3] In this way the low energy hadron

sector of the theories is matched to experiment, and it is natural to expect that the quark masses agree at a relatively low scale. On the other hand we do not want to push the perturbation theory needed for giving $\overline{m}_b$ in the $\overline{\mathrm{MS}}$ scheme to scales below 2 GeV. We remark that also the strange quark mass at 2 GeV is known to be only weakly dependent on $N_f$ [67,68].

In contrast, the RGI mass $M_b$ differs significantly between $N_f = 5$ and $N_f = 2$. Given the observed weak flavour number dependence at scales of 2–5 GeV, the differences in $M_b$ can be traced back to the $N_f$ dependence of both the RG functions and the $\Lambda$ parameters. These two effects happen to reinforce each other between $N_f = 5$ and $N_f = 2$ while in the comparison $N_f = 2$ and $N_f = 0$ they partially compensate.

All of this suggests to use the b-quark mass at scales around $\mu = 2$ GeV when one attempts to make predictions from theories with a smaller number of flavours for the physical 5-flavour theory.

With a less detailed look, the overall picture of the $\overline{\mathrm{MS}}$ masses in Table 4 suggests that – at the present level of errors – the b-quark mass is correctly determined from the different approaches. Our method is very different from those which enter the PDG average. It avoids perturbative errors in all stages of the computation except for the connection of the RGI mass to the running mass in the $\overline{\mathrm{MS}}$ scheme, where truncation errors seem to be very small. Due to these properties, it remains of interest to apply our method with at least three light dynamical quarks and test the consistency of the table once more. As remarked earlier, the error budget of our present computation is such that in a future computation a significantly more precise number can be expected.

## Acknowledgements

## Appendix A. Error propagation and conversion to $\overline{m}(\overline{m})$

Here we give details on the conversion function $\rho(r)$ that has been used in (3.12). It connects the RGI quark mass $M$ to the quark mass $m_*$ defined by $\overline{m}(m_*) = m_*$ and usually denoted by $\overline{m}(\overline{m})$. We closely follow the standard steps which have been outlined in our notation in [70]. In a given scheme our conventions for the RG invariants read

---

[3] For $N_f = 0$ we used the scale $r_0 \approx 0.5$ fm instead of the decay constants, but in [55] this value of $r_0$ was obtained for the $N_f = 2$ theory.

**Table 4**

Masses of the b-quark in GeV in theories with different quark flavour numbers $N_f$ and for different schemes/scales as well as $\Lambda_{\overline{MS}}$ and the RGI mass $M$. The PDG value of the b-quark mass is dominated by [8,24].

| $N_f$ | Ref. | $M$ | $\overline{m}_{\overline{MS}}(\overline{m}_{\overline{MS}})$ | $\overline{m}_{\overline{MS}}(4\,\text{GeV})$ | $\overline{m}_{\overline{MS}}(2\,\text{GeV})$ | $\Lambda_{\overline{MS}}$ [MeV] |
|---|---|---|---|---|---|---|
| 0 | [36] | 6.76(9) | 4.35(5) | 4.39(6) | 4.87(8) | 238(19) [69] |
| 2 | this work | 6.58(17) | 4.21(11) | 4.25(12) | 4.88(15) | 310(20) [55] |
| 5 | PDG13 [1] | 7.50(8) | 4.18(3) | 4.22(4) | 4.91(5) | 212(8) [1] |

$$\frac{\Lambda}{\mu} = \left[b_0 \bar{g}^2(\mu)\right]^{-\frac{b_1}{2b_0^2}} e^{-\frac{1}{2b_0 \bar{g}^2(\mu)}}$$

$$\times \exp\left\{-\int_0^{\bar{g}(\mu)} dg\left[\frac{1}{\beta(g)} + \frac{1}{b_0 g^3} - \frac{b_1}{b_0^2 g}\right]\right\} \equiv \varphi_g(\bar{g}), \quad (A.1)$$

$$\frac{M}{\overline{m}(\mu)} = \left[2b_0 \bar{g}^2(\mu)\right]^{-\frac{d_0}{2b_0}} \exp\left\{-\int_0^{\bar{g}(\mu)} dg\left[\frac{\tau(g)}{\beta(g)} - \frac{d_0}{b_0 g}\right]\right\}$$

$$\equiv \varphi_m(\bar{g}), \quad (A.2)$$

with universal coefficients $b_0 = (11 - 2N_f/3)(4\pi)^{-2}$, $b_1 = (102 - 38N_f/3)(4\pi)^{-4}$ and $d_0 = 8(4\pi)^{-2}$, cf. [65]. From their ratio one obtains a relation

$$r \equiv \frac{M}{\Lambda} = \frac{\overline{m}(\mu)}{\mu} \times \frac{\varphi_m(\bar{g}(\mu))}{\varphi_g(\bar{g}(\mu))} \quad (A.3)$$

that for fixed $\overline{m}(\mu)/\mu$ allows us to parameterize the renormalized coupling $\bar{g}^2(\mu)$ through $r$. Choosing $\mu = m_*$ with $\bar{g}(m_*) = g_*$ in Eq. (A.2) then leads to the functional dependence

$$m_* = M \cdot \rho(r), \quad \text{with } \rho(r) = 1/\varphi_m(g_*). \quad (A.4)$$

We evaluate this function at 4-loop order in the $\overline{MS}$ scheme for $N_f = 2$ flavours and obtain to a very good approximation $\rho(r) = 0.6400 - 0.0043 \cdot (r - 21)$ close to $r = 21$.

Let us now turn to the propagation of errors from the non-perturbative quark mass renormalization and coupling renormalization to $\overline{m}(\overline{m})$. To incorporate correlations among our non-perturbative data for $M$ and $\Lambda$, we write

$$r = \frac{L_0 M}{L_0 \Lambda_{\overline{MS}}} = \frac{L_1 \overline{m}_{SF}(L_0)}{2} \frac{h(L_0)}{k(L_0)}, \quad L_0 = L_1/2, \quad (A.5)$$

where we made use of the definitions $z = L_1 M = L_1 h(L_0)\overline{m}_{SF}(L_0)$ [38] and

$$h(L_0) = \frac{M}{\overline{m}_{SF}(L_0)}, \qquad k(L_0) = \Lambda_{SF} L_0 \cdot \left[\frac{\Lambda_{\overline{MS}}}{\Lambda_{SF}}\right], \quad (A.6)$$

with $\Lambda_{\overline{MS}}/\Lambda_{SF} = 2.382035(3)$. The factors $h(L_0)$ and $k(L_0)$ are determined by the running of the quark mass and the coupling in the Schrödinger Functional (SF) scheme. They are known non-perturbatively in terms of the step scaling functions of [65]. For the error analysis we take the errors in $h, k$ including their correlation into account, remembering that $h$ also contributes through $M_b = h(L_0)\overline{m}_b^{SF}(L_0)$. The uncertainty arising from the perturbative running in the $\overline{MS}$ scheme is negligible. For example, adding the recently computed 5-loop term in the mass anomalous dimension [71] does not change numbers at the one permille level. The error analysis for $\overline{m}_{\overline{MS}}(\mu)$ with some fixed $\mu$ is carried through analogously.

## References

[1] Particle Data Group Collaboration, J. Beringer, et al., Review of Particle Physics (RPP), Phys. Rev. D 86 (2012) 010001, and 2013 partial update for the 2014 edition.

[2] S. Narison, A fresh look into $m_{c,b}$ and precise $f_{D_{(s)},B_{(s)}}$ from heavy–light QCD spectral sum rules, Phys. Lett. B 718 (2013) 1321–1333, arXiv:1209.2023.

[3] S. Bodenstein, J. Bordes, C. Dominguez, J. Penarrocha, K. Schilcher, Bottom-quark mass from finite energy QCD sum rules, Phys. Rev. D 85 (2012) 034003, arXiv:1111.5742.

[4] A. Hoang, P. Ruiz-Femenia, M. Stahlhofen, Renormalization group improved bottom mass from upsilon sum rules at NNLL order, J. High Energy Phys. 1210 (2012) 188, arXiv:1209.0450.

[5] S. Narison, Gluon condensates and $m_b(m_b)$ from QCD-exponential moments at higher orders, Phys. Lett. B 707 (2012) 259–263, arXiv:1105.5070.

[6] A. Laschka, N. Kaiser, W. Weise, Quark–antiquark potential to order $1/m$ and heavy quark masses, Phys. Rev. D 83 (2011) 094002, arXiv:1102.0945.

[7] BABAR Collaboration, B. Aubert, et al., Measurement and interpretation of moments in inclusive semileptonic decays $\bar{B} \to X_c \ell^- \bar{\nu}$, Phys. Rev. D 81 (2010) 032003, arXiv:0908.0415.

[8] K. Chetyrkin, J. Kühn, A. Maier, P. Maierhofer, P. Marquard, et al., Charm and bottom quark masses: an update, Phys. Rev. D 80 (2009) 074010, arXiv:0907.2110.

[9] DELPHI Collaboration, J. Abdallah, et al., Study of b-quark mass effects in multi-jet topologies with the DELPHI detector at LEP, Eur. Phys. J. C 55 (2008) 525–538, arXiv:0804.3883.

[10] Belle Collaboration, C. Schwanda, et al., Measurement of the moments of the photon energy spectrum in $B \to X_s\gamma$ decays and determination of $|V_{cb}|$ and $m_b$ at Belle, Phys. Rev. D 78 (2008) 032016, arXiv:0803.2158.

[11] DELPHI Collaboration, J. Abdallah, et al., Determination of the b quark mass at the $M_Z$ scale with the DELPHI detector at LEP, Eur. Phys. J. C 46 (2006) 569–583, arXiv:hep-ex/0603046.

[12] R. Boughezal, M. Czakon, T. Schutzmeier, Charm and bottom quark masses from perturbative QCD, Phys. Rev. D 74 (2006) 074006, arXiv:hep-ph/0605023.

[13] O. Buchmüller, H. Flächer, Fit to moment from $B \to X_c \ell \bar{\nu}$ and $B \to X_s\gamma$ decays using heavy quark expansions in the kinetic scheme, Phys. Rev. D 73 (2006) 073008, arXiv:hep-ph/0507253.

[14] A. Pineda, A. Signer, Renormalization group improved sum rule analysis for the bottom quark mass, Phys. Rev. D 73 (2006) 111501, arXiv:hep-ph/0601185.

[15] C.W. Bauer, Z. Ligeti, M. Luke, A.V. Manohar, M. Trott, Global analysis of inclusive B decays, Phys. Rev. D 70 (2004) 094017, arXiv:hep-ph/0408002.

[16] A. Hoang, M. Jamin, $\overline{MS}$ charm mass from charmonium sum rules with contour improvement, Phys. Lett. B 594 (2004) 127–134, arXiv:hep-ph/0403083.

[17] J. Bordes, J. Penarrocha, K. Schilcher, Bottom quark mass and QCD duality, Phys. Lett. B 562 (2003) 81–86, arXiv:hep-ph/0212083.

[18] G. Corcella, A. Hoang, Uncertainties in the $\overline{MS}$ bottom quark mass from relativistic sum rules, Phys. Lett. B 554 (2003) 133–140, arXiv:hep-ph/0212297.

[19] M. Eidemüller, QCD moment sum rules for Coulomb systems: The charm and bottom quark masses, Phys. Rev. D 67 (2003) 113002, arXiv:hep-ph/0207237.

[20] J. Erler, M. Luo, Precision determination of heavy quark masses and the strong coupling constant, Phys. Lett. B 558 (2003) 125–131, arXiv:hep-ph/0207114.

[21] CLEO Collaboration, A. Mahmood, et al., Measurement of lepton momentum moments in the decay $\bar{B} \to X \ell \bar{\nu}$ and determination of heavy quark expansion parameters and $|V_{cb}|$, Phys. Rev. D 67 (2003) 072001, arXiv:hep-ex/0212051.

[22] N. Brambilla, Y. Sumino, A. Vairo, Quarkonium spectroscopy and perturbative QCD: Massive quark loop effects, Phys. Rev. D 65 (2002) 034001, arXiv:hep-ph/0108084.

[23] A.A. Penin, M. Steinhauser, Heavy quarkonium spectrum at $\mathcal{O}(\alpha_s^5 m_q)$ and bottom/top quark mass determination, Phys. Lett. B 538 (2002) 335–345, arXiv:hep-ph/0204290.

[24] C. McNeile, C. Davies, E. Follana, K. Hornbostel, G. Lepage, High-precision $c$ and $b$ masses, and QCD coupling from current–current correlators in lattice and continuum QCD, Phys. Rev. D 82 (2010) 034512, arXiv:1004.4285.

[25] ETM Collaboration, P. Dimopoulos, et al., Lattice QCD determination of $m_b$, $f_B$ and $f_{B_s}$ with twisted mass Wilson fermions, J. High Energy Phys. 1201 (2012) 046, arXiv:1107.1441.

[26] G.M. de Divitiis, M. Guagnelli, R. Petronzio, N. Tantalo, F. Palombi, Heavy quark masses in the continuum limit of quenched lattice QCD, Nucl. Phys. B 675 (2003) 309–332, arXiv:hep-lat/0305018.

[27] D. Guazzini, R. Sommer, N. Tantalo, Precision for B-meson matrix elements, J. High Energy Phys. 0801 (2008) 076, arXiv:0710.2229.

[28] N. Carrasco, M. Ciuchini, P. Dimopoulos, R. Frezzotti, V. Gimenez, et al., B-physics from $N_f = 2$ tmQCD: the Standard Model and beyond, arXiv:1308.1851.

[29] A. Gray, I. Allison, C. Davies, E. Dalgic, G. Lepage, et al., The $\Upsilon$ spectrum and $m_b$ from full lattice QCD, Phys. Rev. D 72 (2005) 094507, arXiv:hep-lat/0507013.

[30] A. Hart, G.M. von Hippel, R. Horgan, A. Lee, C.J. Monahan, The b quark mass from lattice nonrelativistic QCD, PoS LATTICE2010 (2010) 223, arXiv:1010.6238.

[31] E. Eichten, B. Hill, An effective field theory for the calculation of matrix elements involving heavy quarks, Phys. Lett. B 234 (1990) 511.

[32] N. Isgur, M.B. Wise, Weak decays in the static quark approximation, Phys. Lett. B 232 (1989) 113–117.

[33] H. Georgi, An effective field theory for heavy quarks at low energies, Phys. Lett. B 240 (1990) 447–450.

[34] E. Eichten, B.R. Hill, Static effective field theory: $1/m$ corrections, Phys. Lett. B 243 (1990) 427–431.

[35] ALPHA Collaboration, J. Heitger, R. Sommer, Non-perturbative Heavy Quark Effective Theory, J. High Energy Phys. 0402 (2004) 022, arXiv:hep-lat/0310035.

[36] M. Della Morte, N. Garron, M. Papinutto, R. Sommer, Heavy Quark Effective Theory computation of the mass of the bottom quark, J. High Energy Phys. 0701 (2007) 007, arXiv:hep-ph/0609294.

[37] B. Blossier, M. Della Morte, N. Garron, R. Sommer, HQET at order $1/m$: I. Non-perturbative parameters in the quenched approximation, J. High Energy Phys. 1006 (2010) 002, arXiv:1001.4783.

[38] B. Blossier, M. Della Morte, P. Fritzsch, N. Garron, J. Heitger, et al., Parameters of Heavy Quark Effective Theory from $N_f = 2$ lattice QCD, J. High Energy Phys. 1209 (2012) 132, arXiv:1203.6516.

[39] R. Sommer, Non-perturbative renormalization of HQET and QCD, arXiv:hep-lat/0209162.

[40] A. Hasenfratz, F. Knechtli, Flavor symmetry and the static potential with hypercubic blocking, Phys. Rev. D 64 (2001) 034504, arXiv:hep-lat/0103029.

[41] A. Hasenfratz, R. Hoffmann, F. Knechtli, The static potential with hypercubic blocking, Nucl. Phys. B, Proc. Suppl. 106 (2002) 418–420, arXiv:hep-lat/0110168.

[42] M. Della Morte, A. Shindler, R. Sommer, On lattice actions for static quarks, J. High Energy Phys. 08 (2005) 051, arXiv:hep-lat/0506008.

[43] B. Blossier, M. Della Morte, G. von Hippel, T. Mendes, R. Sommer, On the generalized eigenvalue method for energies and matrix elements in lattice field theory, J. High Energy Phys. 0904 (2009) 094, arXiv:0902.1265.

[44] M. Lüscher, Solution of the Dirac equation in lattice QCD using a domain decomposition method, Comput. Phys. Commun. 156 (2004) 209–220, arXiv:hep-lat/0310048.

[45] M. Lüscher, Schwarz-preconditioned HMC algorithm for two-flavour lattice QCD, Comput. Phys. Commun. 165 (2005) 199, arXiv:hep-lat/0409106.

[46] M. Lüscher, Deflation acceleration of lattice QCD simulations, J. High Energy Phys. 0712 (2007) 011, arXiv:0710.5417.

[47] M. Lüscher, DD-HMC algorithm for two-flavour lattice QCD, http://luscher.web.cern.ch/luscher/DD-HMC/index.html.

[48] M. Marinkovic, S. Schaefer, Comparison of the mass preconditioned HMC and the DD-HMC algorithm for two-flavour QCD, PoS LATTICE2010 (2010) 031, arXiv:1011.0911.

[49] K.G. Wilson, Confinement of quarks, Phys. Rev. D 10 (1974) 2445–2459.

[50] B. Sheikholeslami, R. Wohlert, Improved continuum limit lattice action for QCD with Wilson fermions, Nucl. Phys. B 259 (1985) 572.

[51] M. Lüscher, S. Sint, R. Sommer, P. Weisz, U. Wolff, Non-perturbative O($a$) improvement of lattice QCD, Nucl. Phys. B 491 (1997) 323–343, arXiv:hep-lat/9609035.

[52] ALPHA Collaboration, S. Schaefer, R. Sommer, F. Virotta, Critical slowing down and error analysis in lattice QCD simulations, Nucl. Phys. B 845 (2011) 93–119, arXiv:1009.5228.

[53] ALPHA Collaboration, U. Wolff, Monte Carlo errors with less errors, Comput. Phys. Commun. 156 (2004) 143–153, arXiv:hep-lat/0306017.

[54] ALPHA Collaboration, S. Lottini, et al., Chiral behaviour of the pion decay constant in $N_f = 2$ QCD, PoS LATTICE2013 (2013) 315.

[55] P. Fritzsch, F. Knechtli, B. Leder, M. Marinkovic, S. Schaefer, et al., The strange quark mass and Lambda parameter of two flavor QCD, Nucl. Phys. B 865 (2012) 397–429, arXiv:1205.5380.

[56] S. Güsken, U. Löw, K. Mütter, R. Sommer, A. Patel, et al., Nonsinglet axial vector couplings of the baryon octet in lattice QCD, Phys. Lett. B 227 (1989) 266.

[57] APE Collaboration, M. Albanese, et al., Glueball masses and string tension in lattice QCD, Phys. Lett. B 192 (1987) 163.

[58] S. Basak, et al., Combining quark and link smearing to improve extended baryon operators, PoS LATTICE2005 (2006) 076, arXiv:hep-lat/0509179.

[59] ALPHA Collaboration, B. Blossier, et al., HQET at order $1/m$: II. Spectroscopy in the quenched approximation, J. High Energy Phys. 1005 (2010) 074, arXiv:1004.2661.

[60] F. Bernardoni, P. Hernandez, S. Necco, Heavy–light mesons in the $\epsilon$-regime, J. High Energy Phys. 1001 (2010) 070, arXiv:0910.2537.

[61] ALPHA Collaboration, J. Bulava, M. Donnellan, R. Sommer, The $B^*B\pi$ coupling in the static limit, PoS LATTICE2010 (2010) 303, arXiv:1011.4393.

[62] J. Gasser, H. Leutwyler, Quark masses, Phys. Rep. 87 (1982) 77–169.

[63] K. Chetyrkin, A. Retey, Renormalization and running of quark mass and field in the regularization invariant and $\overline{\text{MS}}$ schemes at three loops and four loops, Nucl. Phys. B 583 (2000) 3–34, arXiv:hep-ph/9910332.

[64] K. Melnikov, T. van Ritbergen, The three loop relation between the $\overline{\text{MS}}$ and the pole quark masses, Phys. Lett. B 482 (2000) 99–108, arXiv:hep-ph/9912391.

[65] ALPHA Collaboration, M. Della Morte, et al., Non-perturbative quark mass renormalization in two-flavor QCD, Nucl. Phys. B 729 (2005) 117–134, arXiv:hep-lat/0507035.

[66] ALPHA Collaboration, B. Blossier, et al., HQET at order 1/m: III. Decay constants in the quenched approximation, J. High Energy Phys. 1012 (2010) 039, arXiv:1006.5816.

[67] G. Colangelo, S. Dürr, A. Jüttner, L. Lellouch, H. Leutwyler, et al., Review of lattice results concerning low energy particle physics, Eur. Phys. J. C 71 (2011) 1695, arXiv:1011.4408.

[68] S. Aoki, Y. Aoki, C. Bernard, T. Blum, G. Colangelo, et al., Review of lattice results concerning low energy particle physics, arXiv:1310.8555.

[69] ALPHA Collaboration, S. Capitani, M. Lüscher, R. Sommer, H. Wittig, Nonperturbative quark mass renormalization in quenched lattice QCD, Nucl. Phys. B 544 (1999) 669–698, arXiv:hep-lat/9810063.

[70] R. Sommer, Introduction to non-perturbative Heavy Quark Effective Theory, arXiv:1008.0710.

[71] K. Chetyrkin, et al., talk presented at the 20th meeting of the SFB/TR 9, 2013.